3D GPR characterization of sandy mouth bars in an outcrop reservoir analog: Cretaceous Ferron Sandstone, south-east Utah

Azie A. Aziz, Robert R. Stewart, Mohammad S. Ullah, University of Houston; Janok P. Bhattacharya, McMaster University*

Summary

Outcrop analog studies have periodically been used to understand the complex sedimentology and stratigraphy of subsurface reservoir architecture for accurate well placement and enhanced oil recovery (EOR) planning during field development. Ground-penetrating radar (GPR) has greatly facilitated analog outcrop study progress as it is relatively high resolution, inexpensive, quick, and has a several meter depth of penetration. A 3D GPR survey was conducted to visualize architectural elements of friction-dominated distributary mouth bars within proximal delta front deposits in Cretaceous Ferron Sandstone at the top of the Notom Delta in south-east Utah. Sensors and Software's Noggin SmartCart 250 MHz was used over a 25 m x 15 m grid. We employed an orthogonal acquisition geometry and a spatial sampling of 0.5 m for the inline (dip direction) and 1.5 m for the crossline (strike direction). Standard processing flows including time-zero correction, dewow, gain, background subtraction and 2D migration were used to increase the signal-to-noise ratio. Formation velocity estimates from the hyperbola matching yielded 0.131 m/ns which is comparable to the literature velocity of about 0.125 m/ns. The calculated average dielectric constant (directly related to volumetric water content) is 5.2 matches unsaturated sandstone. The depth of GPR penetration is limited to approximately 3 m - likely due to the compaction/carbonate cementation in the rock and interbedded layers of finer-grained material contributing to higher attenuation of the GPR signal. The vertical resolution is about 0.125 m, enabling the imaging of the dune-scale cross sets (15-20 cm thickness). Calculation of the medium porosity via an adapted Wyllie Time Average equation yields 7.8 % which is consistent with the average porosity (5-10%) obtained from the literature. Bedding diagrams from local cliff exposures show gently NE dipping accretion of single large foresets that were interpreted as small scale unit bars, which are the building blocks of the large mouth bars. The GPR radargrams are not only capable to image that, but also reveals their 3D shape. A closer look into GPR images also reveals the distinction between various proximal mouth bar facies: upper friction-dominated dune-scale cross beds and bar scale large foresets from lower inertia-dominated basal planar beds.

Introduction

GPR is an emerging technology for mapping the geometries of the outcrop analogs to characterize the complicated architecture of a buried 3D reservoirs (Corbeanu et al., 2001; Flint and Bryant, 1993). Outcrop geophysical properties are assumed to be representative of those (velocity, porosity, etc.) in the subsurface (Jarrard et al., 2004). For analog studies, surface seismic data is excellent in sampling the whole reservoir geometry but it is often lacking in the resolution to visualize the geobody (Howell et al., 2014). Well data are sparse and we tend to interpolate data between available wells and this is a rather inaccurate representation of the lateral variation of the reservoir architecture. GPR provides a solution of acquiring high-resolution of shallow subsurface reservoir with wavelengths in the range of centimeters (Asprion and Aigner, 1997). In addition, GPR is efficient in mapping lithofacies because it offers real-time output and requires minimal processing (Bridge, 2003)

GPR is useful to study stratasets because the sedimentary character strata can be interpreted from the radar reflections (Bridge, 2003). GPR is ideal in studying the outcrop analog of Cretaceous Ferron Sandstone because of the little clay or silt presence. Clay-rich materials are highly attenuating and limit the GPR depth of penetration. The objectives of the study are to acquire GPR data from Cretaceous Ferron sandstone outcrops, extract the geophysical information such as the velocity, depth of penetration, vertical resolution, porosity and reconstruct a 3-D facies architecture model for the distributary mouth bars. Also, we would like to describe the geometry and the distribution of the facies architecture observed on the radargram after processing.

Survey location and geological setting

The study area is located in the Coalmine Wash area, near Hanksville in south-east Utah (Fig.1). The Cretaceous Ferron Sandston (member of the Mancos Shale Formation) was one of the deltaic systems in a series of northeast-prograding clastic wedges (Li and Bhattacharya, 2013; Ryer and Anderson, 2004). It is an important study area as it is considered as a hydrocarbon reservoir analog (McMehan et al., 1997; Szerbiak et al., 2001; Corbeanue et al., 2004). The Ferron sandstone is an example of a reservoir analog for some of the most productive oil fields in the Gulf of Mexico, Alaskan North Slope, North Sea and Rocky Mountain Basin. It is an example of river- and wave-dominated deltaic

DOI http://dx.doi.org/10.1190/segam2015-5917183.1

reservoirs which are some of the largest untapped and unrecovered reservoirs in the world.

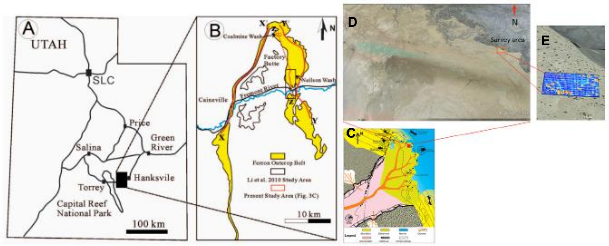

Figure 1: Basemap A shows Utah and basemap B shows the location of the study area marked with a black rectangle (Li et al., 2014). The Google Earth images D and E show the GPR grid location and the GPR depth slice overlain on the grid respectively, (adapted from Li and Bhattacharya, 2013).

The survey location has some excellent exposures of delta facies for a margin of subsiding basin (Fig.2). With established sequence stratigraphic framework, the survey location is ideal for GPR work. The Ferron sandstone is the source of the most active gas play in Utah. Ferron coalbed methane reported to have 10 TCF of gas reserves (Gloyn and Sommer, 1993).

Figure 2: Photograph of the survey location. Note the excellent, extensive and continuous exposure of high quality outcrop of the Ferron sandstone ideal for GPR survey. The GPR survey crew can be seen at a distant.

Previous studies (for example: Ahmed et al., 2014; Li et al., 2014) documented the river-dominated distributary mouth bars as an essential building blocks of Ferron deltaic wedge. Fig. 3 shows distributary mouth bars form when river enters standing body of water and become unconfined, depositing sediments at river mouth (Li et al., 2014).

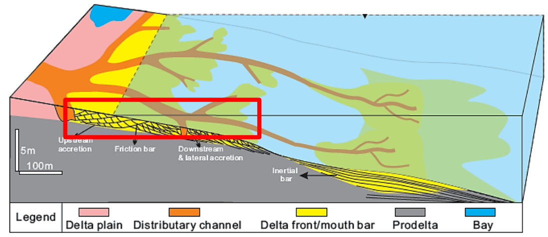

Figure 3: The distributary mouth bar (red box) model depicted by Li and Bhattacharya (2013).

In this work, we are focusing on Parasequence 6 of sequence 2 marked by "Distributary mouth bar" shown in Fig. 4. Fig. 4 shows a regional dip cross-section through the Ferron Notom delta system shows different parasequences (Zhu, 2010; Zhu et al., 2012). In the Ferron sandstone, parasequences may be considered as primary reservoir building blocks because marine and delta-plain shales act as laterally extensive permeability barrier. Some communication may be established between parasequence because of erosion of the shale.

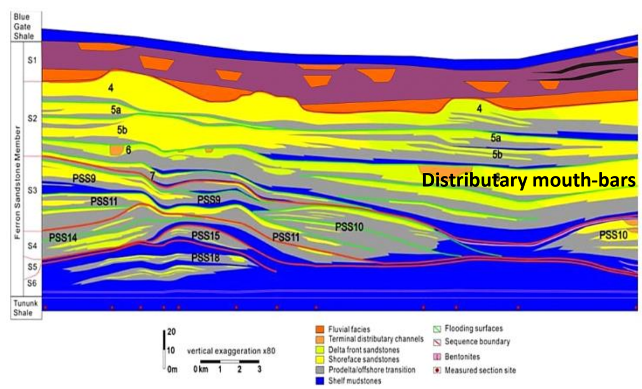

Figure 4: Oblique depositional strike sequence stratigraphy of the Notom delta by Li, (2009) shows the distributary mouth bar located in parasequence 6 of sequence 2 which is the focus of this study.

Data acquisition

A 3-D common-offset GPR data set were acquired using Sensors and Software's Noggin Plus SmartCart 250 MHz (Fig. 5). We acquired GPR lines in the inline (dip direction)

DOI http://dx.doi.org/10.1190/segam2015-5917183.1

Figure 5: Rectangular grid (25 m x 15 m) of 3D GPR data acquisition using Sensors and Software's Noggin Plus SmartCart 250 MHz antenna on the top of the outcrop analog.

and the crossline (strike direction). Data acquisition was undertaken in a parallel forward-reverse procedure to provide efficient acquisition. This survey orientation should provide well-sampled in-line data. A 25 m by 15 m survey grid was designed on the outcrop (Figure 6).

An XY forward and reverse collection method was employed to obtain an orthogonal survey grid. Inline sampling was 0.5 m while crossline was 1.5 m. The details of the survey parameters are shown in Table 1.

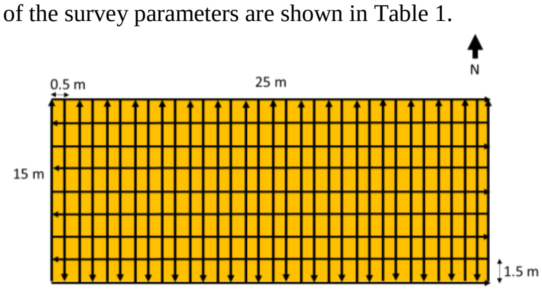

Figure 6: A forward and reverse collection method was employed to obtain an orthogonal survey grid.

Parameter	Value
Center frequency	250 MHz
Line spacing	0.5 m (inline) 1.5 m (crossline)
Step size	0.1 m
Vertical stacking	64
Sample rate	0.40 ns
Antenna separation	0.27 m

Table 1: GPR survey parameters at the geophsyical test site.

Data processing and analysis

GPR data processing was undertaken using Sensors & Software processing package EKKOView Deluxe. The main steps are: time-zero correction, dewow, spherical and exponential compensation (SEC) gain, bandpass filtering, background removal, and 2D migration.

The 250 MHz GPR data set gives a vertical resolution (~0.125 m) with an approximated penetration depth of about 3m. The depth of penetration is enough to interpret the top of the Proximal delta front. For depth conversion, we estimated the GPR velocity using hyperbola matching method and from the literature. The hyperbola matching technique gave a velocity of 0.131 m/ns while literature reported a velocity of typical dry sandstone is 0.125 m/ns (Lee et al., 2007). We used a constant velocity of 0.125 m/ns in the 2D migration for geological interpretation.

From the measured radar velocity, we estimate the formation porosity by using the Wyllie Time-Average equation (1) (Aitken, 2008).

$$\frac{1}{V_A} = \frac{\emptyset}{V_F} + \frac{1-\emptyset}{V_M} \quad (1)$$

where $\emptyset$ is the porosity, V_A is the measured radar velocity (0.131 m/ns), V_F is the fluid velocity (air = 0.3 m/ns) within the pore space, and V_M is the rock matrix velocity (0.125 m/ns). The calculation yields 7.83 % which is in the range of the reported average porosity of the Ferron sandstone (5-10 %). The calculated porosity can be used to calculate the radar velocity of saturated sandstone. We used 0.033 m/ns to represent the fluid velocity, V_F (Aitken, 2008). The velocity of water saturated sandstone is 0.103 m/ns which is in the range of wet sandstone (0.09-0.13 m/ns) reported in the literature (Bakker et al., 2007).

The calculated average dielectric constant (directly related to volumetric water content) is 5.2 matches unsaturated sandstone.

GPR interpretation

The GPR radargrams help to image and reveal the 3D shape of the sandstone. Detailed assessment of the GPR images also assists in making distinctions between various proximal mouth bar facies: upper friction-dominated dune-scale cross beds and bar-scale large foresets from lower inertia-dominated basal planar beds.

In Fig.7, the top parallel reflectors (upper 40 cm) represents dune-scale cross beds on top of a unit bar consisting of steeply dipping bar scale single large foresets typically 5-15 cm thick. The flow direction is not clear as the GPR is unable to resolve individual cross stratifications. However, the reflector boundaries may indicate the 1st or 2nd order cross set/co-set boundaries that may reflect a change is grain-size between successive cross sets. The apparent vertical lines in the top 40 cm may arise from data gathering errors due to surface undulation and/or vegetational cover. The lower part of the mouth bar shows coherent planar beds. The lower part

DOI http://dx.doi.org/10.1190/segam2015-5917183.1

of the mouth bar is interpreted as coherent planar beds deposited in higher water depth.

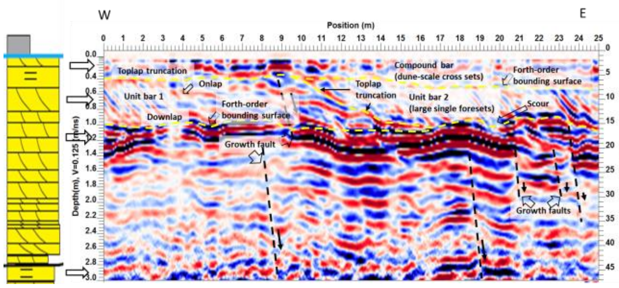

Figure 7: GPR image shows the upper dune-scale cross beds interpreted to be deposited in a friction-dominated environment. Estimated deposited subaqueously, in water depth no more than few meters.

Fig. 8 shows a dune-scale cross sets of about 30 cm thick on top of a progradational mouth bar. The progradational mouth bar is characterized by large single foresets are typically deposited as friction-dominated shows a dip angle of 50 degree. We observed progradational unit mouth bar which has large single foresets which is charaterized by oblique, high amplitude and continuous reflection. Bed height is about 0.8 m which is translated to channel width. Small-scale undulations and laterally continuous basal planar beds are observed in Fig. 8. The lateral planar beds are interpreted to be deposited in an inertia-dominated river mouth during a flood event, similar to those described by Martinsen et al. (1990). These planar beds lie about 10 m below the top of parasequence 6 (a flooding surface), and were probably deposited in a water depth of about 10 m, which favors the dominance of inertial forces.

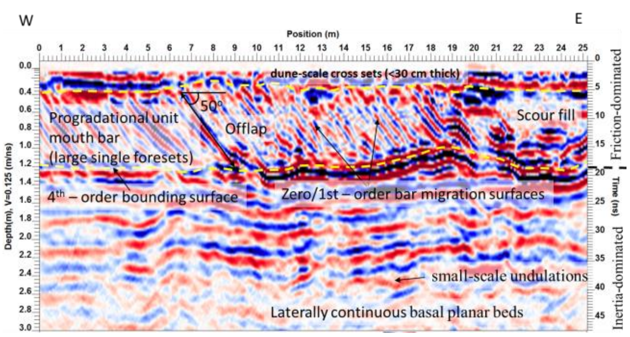

Figure 8: GPR image shows the progradational unit mouth bar with a dip angle of 50 degrees deposited by friction-dominated river flow. The laterally continuous basal planar bed at the bottom of the figure is interpreted to be deposited in an inertia-dominated river mouth during a flood event.

Fig. 9 is shows GPR image in strike-direction. It displays a terminal distributary channel deposit with a depth of 1.5 m. The channel is characterized by a basal erosional surface and occurs at the upper part of the coarsening upward succession. The basal erosional surface is deposited as friction dominated. We also observed dune-scale cross-bedded sandstone.

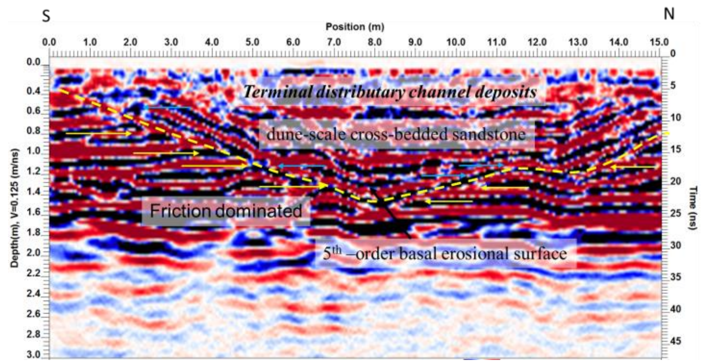

Figure 9: GPR image GPR image in strike-direction. It displays a terminal distributary channel deposit with a depth of 1.5 m.

We visualized the terminal distributary channel by analyzing the successive 3D cube of GPR profiles using the 3D Voxler software shown in Fig.10.

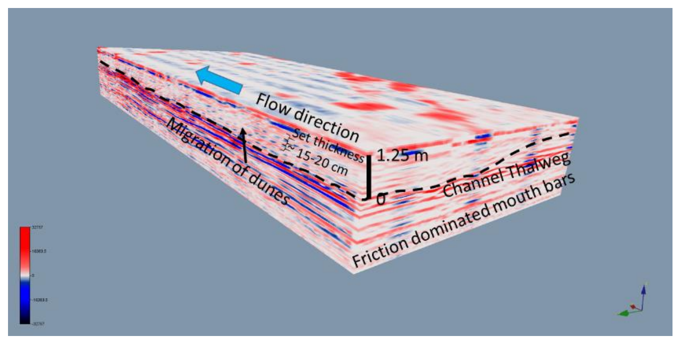

Figure 10: GPR image GPR image in strike-direction. It displays a terminal distributary channel deposit with a depth of 1.5 m.

Conclusions

The 3D GPR data, over the 25 m x 15 m grid, were acquired to augment the available sedimentological and stratigraphic information of a river-dominated mouth bar reservoir analogue in the Ferron Sandstone, Notom Delta, Utah. The 250 MHz GPR data have a vertical resolution of some 12.5 cm and depth of penetration of about 3 m. The GPR data assist in reconstructing the 3D geometry of the sand bars. Additional information like velocity, relative dielectric constant and porosity was also derived.

Acknowledgements

We would like to thank the Allied Geophysical Lab team, especially Long Huang, for acquiring the GPR data and supporting the investigation.

DOI http://dx.doi.org/10.1190/segam2015-5917183.1

EDITED REFERENCES

Note: This reference list is a copyedited version of the reference list submitted by the author. Reference lists for the 2015 SEG Technical Program Expanded Abstracts have been copyedited so that references provided with the online metadata for each paper will achieve a high degree of linking to cited sources that appear on the Web.

REFERENCES

Ahmed, S., J. P. Bhattacharya, D. Garza, and Y. Li, Construction of an inertia- to friction-influenced delta front, Turonian Ferron Sandstone, Utah: Journal of Sedimentary Research.

Aitken, J. A., 2008, Exploring Maya ruins in Belize, Central America using ground-penetrating radar (GPR): M.S. thesis, University of Calgary.

Asprion, U., and T. Aigner, 1997, Aquifer architecture analysis using ground-penetrating radar:Triassic and quaternary examples: Environmental Geology, **31**, no. 1-2, 66–75. http://dx.doi.org/10.1007/s002540050165.

Bakker, M. A. J., D. Maljers, and H. J. T. Weerts, 2007, Ground-penetrating radar profiling onembanked floodplains: Netherlands Journal of Geosciences, **86**, 55–61.

Bridge, J. S., 2003, Rivers and Floodplains: Blackwell, 491 p.

Corbeanu, R. M., K. Soegaard, R. B. Szerbiak, J. B. Thurmond, G. A. McMechan, D. Wang, S. H. Snelgrove, C. B. Forster, and A. Menitove, 2001, Detailed internal architecture of fluvial channel sandstone determined from outcrop and 3-D ground penetrating radar: Example from mid-Cretaceous Ferron Sandstone, east-central Utah: AAPG Bulletin, **85**, 1583–1608.

Corbeanu, R. M., M. C. Wizevich, J. P. Bhattacharya, X. Zeng, and G. A. McMechan, 2004, Three-dimensional architecture of ancient lower delta-plain point bars using ground-penetrating radar, Cretaceous Ferron Sandstone, Utah, *in* T. C. Chidsey Jr., R. D. Adams, and T. H. Morris, eds., Regional to Wellbore Analog for Fluvial-deltaic Reservoir Modeling: The Ferron Sandstone of Utah, AAPG Studies in Geology No. 50, 427–449.

Flint, S. S., and D. Bryant, 1993, The geological modeling of hydrocarbon reservoirs and outcrop analogs: Blackwell.

Gloyn, R. W., and S. N. Sommer, 1993. Exploration for coalbed methane gains momentum in Uinta Basin, Utah Geological Survey: Oil & Gas Journal, Exploration, 73–76.

Howell, J. A., A. W. Martinius, and T. R. Good, 2014, The application of outcrop analogues in geological modelling: A review, present status and future outlook, *in* A. W. Martinius, J. A. Howelll and T. R. Good, eds., Sediment-Body Geometry and Heterogeneity: Analogue Studies for Modelling the Subsurface: The Geological Society 387, 1–25.

Jarrard, R. D., C. H. Sondergeld, M. A. Chan, and S. N. Erickson, 2004, Petrophysics of the Cretaceous Ferron Sandstone, Central Utah: AAPG Studies in Geology, **50**, 227–249.

Lee, K., M. Tomasso, W. A. Ambrose, and R. Bouroullec, 2007, Integration of GPR with stratigraphic and lidar data to investigate behind-the-outcrop 3D geometry of a tidal channel reservoir analog, upper Ferron Sandstone, Utah: The Leading Edge, **26**, 994–998. http://dx.doi.org/10.1190/1.2769555.

Li, Y., and J. P. Bhattacharya, 2013, Facies architectural study of a stepped, forced regressive compound incised valley system in the Ferron Notom Delta, Southern Utah: Journal of Sedimentary Research, **83**, no. 3, 206–225. http://dx.doi.org/10.2110/jsr.2013.19.

Li, Y., and J. P. Bhattacharya, 2014, Facies architecture, branching pattern, and paleodischarge of a lower Delta-Plain distributary channel system in the Cretaceous Ferron Notom Delta, Southern Utah, U.S.A: Sedimentology, **61**, 1452–1483. http://dx.doi.org/10.1111/sed.12104.

DOI http://dx.doi.org/10.1190/segam2015-5917183.1

McMechan, G. A., G. C. Gaynor, and R. B. Szerbiak, 1997, Use of ground-penetrating radar for 3-D sedimentological characterization of clastic reservoir analogs: Geophysics, **62**, no. 3, 786–796. http://dx.doi.org/10.1190/1.1444188.

Ryer, T. A., and P. B. Anderson, 2004, Facies of the Ferron Sandstone, East-Central Utah in regional to wellbore analog for Fluvial–Deltaic reservoir modelling: The Ferron Sandstone of Utah, *in* Chidsey, T. C., R. D. Adams, and T. H. Morris, eds.: AAOG, Studies in Geology, 50: 59–78.

Szerbiak, R. B., G. A. McMechan, R. M. Corbeanu, C. Forster, and S. H. Snelgrove, 2001, 3-D characterization of a clastic reservoir analog: From 3-D GPR to a 3-D fluid permeability model: Geophysics, **66**, no. 4, 1026–1037. http://dx.doi.org/10.1190/1.1487050.

Zhu, Y., 2010, Sequence Stratigraphy and facies architecture of the Cretateous Ferron Notom Delta Complex, South-Central Utah, U.S.A.: PhD Dissertation, University of Houston, 128p

Zhu, Y., J. P. Bhattacharya, W. Li, T. J. Lapen, B. R. Jicha, and B. S. Singer, 2012, Milankovitch-scale sequence stratigraphy and stepped forced regressions of the Turonian Ferron Notom deltaic complex, south-central Utah, U.S.A: Journal of Sedimentary Research, **82**, no. 9, 723–746. http://dx.doi.org/10.2110/jsr.2012.63.